Water-tolerant SBA-16 confined phosphotungstic acid for controllable synthesis of jet fuel blending with cyclic ketones

Yanan Liu[a], Genkuo Nie*[b], Shitao Yu[b], Ji-Jun Zou[a], Lun Pan[a], Li Wang[a], Xiangwen Zhang[a] and Chengxiang Shi*[a]

a Key Laboratory for Green Chemical Technology of the Ministry of Education, School of Chemical Engineering and Technology, Tianjin University; Collaborative Innovative Center of Chemical Science and Engineering (Tianjin), Tianjin 300072, China

b State Key Laboratory Base of Eco-chemical Engineering, College of Chemical Engineering, Qingdao University of Science and Technology, 53 Zhengzhou Road, Qingdao 266042, China

Corresponding author. Tel and fax: 86-22-27892340. E-mail: niegenkuo@qust.edu.cn, cxshi@tju.edu.cn (Chengxiang Shi).

Abstract

Transferring lignocellulose-derived ketones to jet fuel blending through aldol condensation has great potential for the synthesis of high-performance jet fuels. However, the water formed in reaction decreases the activity of catalyst, especially the acid catalyst. Herein, water-tolerant SBA-16 confined phosphotungstic acid was developed to be applied in this reaction with high performance. The SBA-16-like pore size was regulated and the surface was modified by alkylimidazole which improves the water-tolerant property of catalyst by creating relative hydrophobic environment and leads to the resistance of HPW leaching and keeping stable performance of the catalyst in 5 runs of aldol condensation. About 64.2% primary-condensation products and 27.8% secondary-condensation products were produced by this catalyst. After hydrodeoxygenation, a high-performance fuel blending with density of about 0.905 g/mL and freezing point of -67 ºC was obtained. This study provides a promising water-tolerant catalyst to develop a new route to produce high-performance bio-jet fuel blending.

Key words: high-density fuel; phosphotungstic acid; SBA-16; aldol condensation; biomass

1. Introduction

Developing biofuel, especially bio-jet fuel is significant as response to the concerns on the depletion of fossil energy and global warming. High-density jet fuel is used in volume limited vehicles to extend the voyage range and load in high space, which demands the fuel to have both high density and good low-temperature properties. To afford high density, jet fuel must have special structures such as polycyclic structure, while to afford good low-temperature properties, jet fuel must limit the carbocyclic ring numbers. To date, the synthesis of jet fuel using lignocellulose derivatives has been intensively studied[1,2] by alkylation[3-6], aldol condensation[7], oligomerization[8], Michael addition[9], Diels-Alder reaction[10] and so on, depending on the biomass derivatives used. Ketones are common compounds from lignocellulose, such as acetone, isophorone, cyclopentanone and cyclohexanone that are intensively used to synthesize jet fuel via aldol condensation. For example, branched cyclic alkanes are synthesized by aldol condensation of furfural (or 5-hydroxymethylfurfural) with cyclopentanone[11], aldol condensation of furfural (or 5-hydroxymethylfurfural) with isophorone[12] and aldol condensation and Michael addition of methyl ketones[13]. Bicyclic hydrocarbons are synthesized by aldol condensation of cyclopentanone or cyclohexanone[14]. However, these fuels synthesized have either high density or low-temperature properties. Therefore, blended fuel with multiple hydrocarbons is more preferred because it provides both high density and low-temperature properties by balancing different compositions[6,15].

Aldol reaction in industry is mostly catalyzed by homogeneous basic[16] and acid[17] catalysts, which suffer from serious problems such as corrosion, difficulties in separation, non-recyclability and high cost in wastewater treatment. To overcome these drawbacks, heterogeneous basic catalysts, such as CaO[18] and MgO[7], are developed, but they are sensitive to CO_2 and water. Acid-base catalysts and solid acid catalysts, such as MgAl-HT[19], heteropolyacids[14], metal oxides[20-22], mesoporous silica[23], and zeolites[24,25] have also been studied to improve aldol condensation. The results show that the stronger acidity of catalyst, the more favorable for the reaction. Among them, the acid strength of phosphotungstic acid (HPW) is stronger than H_2SO_4[26]. However, the surface area of HPW is low (5 m^2/s), so HPW loaded on porous supports has been applied to enhance the catalytic activities and selectivity

through increasing the amount of effective sites and creating confined reaction environment[14,27]. Porous supports such as mesoporous silica are desirable for pore size adjustable and can be used to control condensed products distribution by size selectivity. Additionally, addressing mass transfer and coke problems, 3D pore network structure is better than one-dimensional ones, for example, SBA-16 is better than SBA-15[28]. Although loaded catalyst systems exhibit good activity, aldol reaction involves dehydration to enone groups and produces water, reducing the acidity of catalyst by acid leaching effect[29]. To solve this problem, incorporation of hydrophobic organic groups in pores of silica were developed to create a hydrophobic environment to protect the acid sites and improve the catalyst activity stability by enhancing the water-tolerance of catalyst[30,31]. The commonly used hydrophobic organic groups are ultra-long alkyl chains and halogenated alkanes[30,31]. Among them, halogenated alkanes can be further quaternized by alkylimidazole to form imidazelium halogenides which could occur ion exchange reaction as anion anchor points and the alkylimidazole as hydrophobic groups protect the anionic ions from leaching[32,33].

With these considerations, in this work we synthesized water-tolerant SBA-16 confined HPW catalyst by alkylimidazole grafting and used it to controllably catalyze cyclic ketones to obtain jet fuel blending. We synthesized SBA-16 using hydrothermal method and modified the surface by 3-chloropropyltrimethoxysilane and then further constructed surface imidazolium halogenides with 1-butylimidazole by quaterisation. HPW was loaded by anionic exchange between imidazolium halogenides and HPW to form water-tolerant SBA-16 confined HPW catalyst. In the continuation of this study, we wish to disclose the excellent catalytic performance of this catalyst in aldol condensation of cyclic ketones to produce excellent jet fuel blending.

2. Experimental

2.1 Materials

Unless stated, all chemicals (AR) and catalysts in this work were used directly after purchasing without any purification. Polymer of methyloxirane and oxirane (F127) was purchased from 3A Chemicals Co., Ltd. Tetraethoxy silicone (TEOS) and ethyl acetate were purchased from Shanghai Aladdin Bio-Chem Technology Co., Ltd. Propylene oxide ethylene oxide block polymer (P123), 3-chloropropyltrimethoxysilane and 1-butylimidazole were

purchased from Shanghai Titan Scientific Co., Ltd. Phosphotungstic acid (HPW) was purchased from Shanghai Xian-Dinn Biotech Co., Ltd. Hydrochloric acid was purchased from Real & Lead Chemical Co., Ltd. Cyclopentanone was purchased from Shanghai Macklin Biochemical Co., Ltd. Cyclohexanone and silicotungstic acid ($H_4SiW_{12}O_{40}$) was purchased from Tianjin Kemiou Chemical Reagent Co., Ltd. Palladium dichloride ($PdCl_2$, 99%) was obtained from Tianjin Guangfu Fine Chemical Research Institute. Hβ (SiO_2/Al_2O_3 = 25) was obtained from Nankai Catalysts Co., Ltd. and calcined in air at 580 ºC for 3 h, and 5 wt% Pd/ Hβ was prepared by impregnation technique[34].

2.2 Synthesis of catalysts

The water-tolerant SBA-16 confined HPW was prepared by three steps (**Figure 1**). Firstly, the SBA-16 as support was prepared through hydrothermal reaction with F127 (and P123) as structure-directing agent, TEOS as silica source, and 3-chloropropyltrimethoxysilane as surface functionalized groups co-condensed with TEOS (**step 1**). Then, the surface halogenated alkane was quaternized with 1-butylimidazole to form imidazolium halogenides as anchors for HPW immobilization (**step 2**). Lastly, HPW was loaded by anion ions exchange with imidazolium halogenides (**step 3**). For example, the HPW/SBA-16-P123-hp samples were prepared as follows: 1.35 g of F127 was dissolved in an aqueous hydrochloric acid solution (67 mL, 0.4 M HCl). After complete dissolution, 0.27 g P123 was added. Then, 6.4 g of TEOS was added at 40 ºC. The mixture was stirred for 10 h and then added with 1.5 g 3-chloropropyltrimethoxysilane, and stirred for 14 h. Subsequently, the mixture was transferred into hydrothermal reaction vessel and crystallized at 100 ºC for 24 h. Then, the solid was filtrated, washed with water, and dried overnight at room temperature. The extra template was removed by Soxhlet extractor with ethanol at 120 ºC for 72 h, and then dried under vacuum at 60 ºC for 10 h. Then the samples were quaternary ammonized with 4.69 g of 1-butylimidazole at 75 ºC for 24 h in 50 mL ethyl acetate. The quaternized samples were filtered and dried under vacuum at 60 ºC. At last, the dried samples were impregnated with 50 mL HPW ethanol solution (15.7 mmol/L). After filtration, washing with alcohol and drying, HPW/SBA-16-P123-hp was obtained and the loaded amount of HPW was analyzed by ICP-OES. Similarly, the sample synthesized with only F127 as structure-directing agent is named

as HPW/SBA-16-hp. The sample synthesized with only F127 and without alkylimidazole grafting is named as HPW/SBA-16.

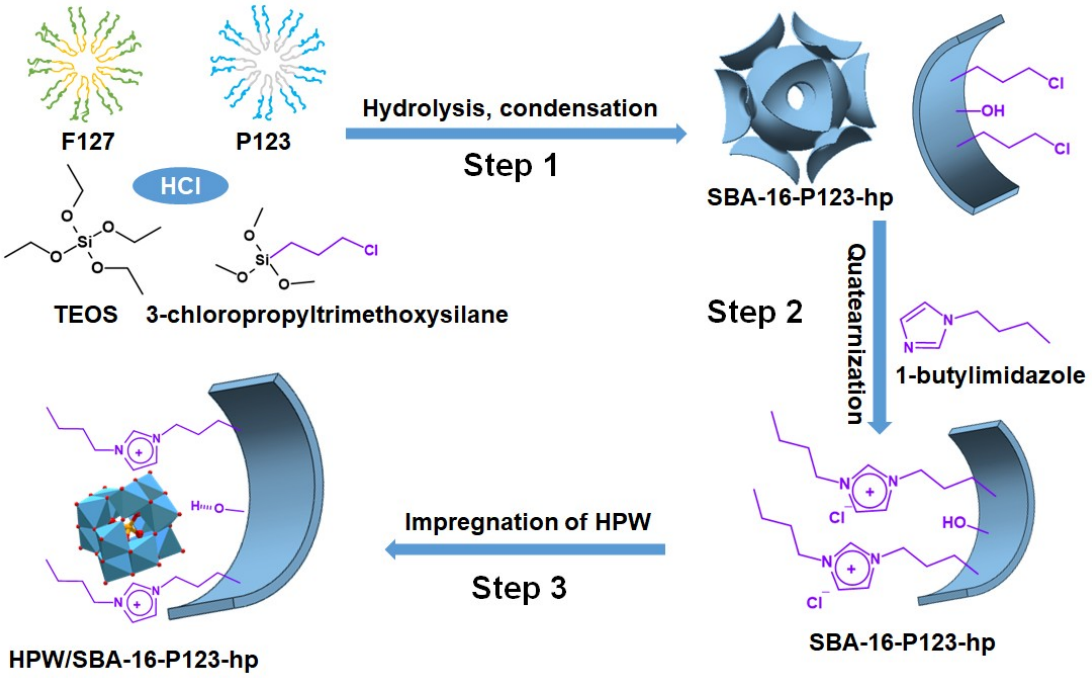

Figure 1 Schematic representation outlining synthesis procedure of the HPW/SBA-16-P123-hp.

2.3 Catalyst characterization

The XRD was conducted on a Rigaku D/MAX-2500 with Kα ray from Cu target, and the tube voltage was 40 kV. The wide-angle XRD was operated with the scan range of 5~80 ° and the scan speed of 4 °/min. The small-angle XRD was operated with the scanning range of 0.5~5 ° and the scan speed of 0.2 °/min. The FT-IR was conducted on a Bruker Vertex 70 with resolution of 4 min^{-1} and wavelength range of 400~4000 cm^{-1}. The scanning electron microscope (SEM) was conducted on QUANTA Q400/cold field S4800 of American FEI company, with the gold sputtering treatment. The transmission electron microscope (TEM) was conducted on a G2 F20 of American FEI company with 200 kV test voltage. TG-DTG was conducted on a TA TGA Q500 in temperature range from 30 ℃ to 800 ℃ in air with an increasing rate of 10 ℃/min to detect the thermal stability of catalyst. Nitrogen adsorption-desorption analysis was conducted to characterize the pore and surface area of the catalysts on a Micromeritics ASAP 2020 at liquid nitrogen temperature (-196 ℃) after degassing the samples at 100 ℃ in vacuum for 10 h. The specific surface areas and pore size distributions

were evaluated by the BET and BJH methods, respectively. ICP-OES was conducted on a Varian VISTA-MPX to analyze the W content. The contact angle test of catalysts was conducted on a JC2000D2M produced by Shanghai Zhongchen Digital Technic Apparatus Co., Ltd.

2.4 Reaction and analysis

For the aldol condensation, 8.14 g (96.8 mmol) cyclopentanone, 9.50 g (96.8 mmol) cyclohexanone and 1.0 g catalyst were added into a 50 mL autoclave (WCGF-50 mL) and the reaction was conducted at 160 ºC for 32 h under N_2 atmosphere. The products were analyzed by an Agilent 6890/5975 gas chromatography-mass spectrometry (GC-MS) equipped with HP-5 capillary column (30 m × 0.5 mm), and an Agilent 7820A gas chromatograph equipped with HP-1 capillary column (30 m × 0.53 mm) and a hydrogen flame ionization detector (FID). The aldol condensation products were hydrodeoxygenated with 5 wt% Pd/Hβ (4 g catalyst/25 g condensed products) at 250 ºC and 6 MPa of H_2 for 3 days in a 50 mL autoclave (EasyChem E50) with mechanical stirring.

2.5 Fuel properties

Mettler Toledo DE40 density meter (ASTM D4052), capillary viscometer (ASTM D445), and the IKA-C6000 isoperibol Package 2/10 Calorimeter (ASTM D240-02) were used to test the density, kinematic viscosity, and net heat of combustion (NHOC) of the products, respectively. The freezing point was measured as outlined in ASTM D2386.

3. Results and Discussion

3.1 Structural characteristics of catalyst

The small-angle X-ray diffraction spectra of the samples are shown in **Figure 2a**. All these samples have a main peak at about 2θ = 0.8 ° and additional peaks at 2θ = 1.0~2.4 ° corresponding to the crystal plane index of (110), (200), (211), (220), (310), (222) respectively[35], indicative of the characteristics of ordered mesoporous of SBA-16. In the wide range of XRD patterns (**Figure 2b**), samples show a broad peak in the range of 2θ = 15~40 ° which is similar with the SBA-16. No separated phase observed in all the samples except HPW/SBA-16, suggesting even dispersion of HPW on SBA-16 with surface alkylimidazole grafting. These ordered mesoporous characters of samples can also be seen in the well-ordered pore structure of TEM (**Figure 2c-d**). Moreover, the elemental mapping images

(**Figure 2e-g**) present the highly uniform distribution of N, P and W, indicating alkylimidazole grafted uniformly and HPW well distributed. Crystal size is shown in SEM micrographs (**Figure 2h**) that the particles are about 10 μm.

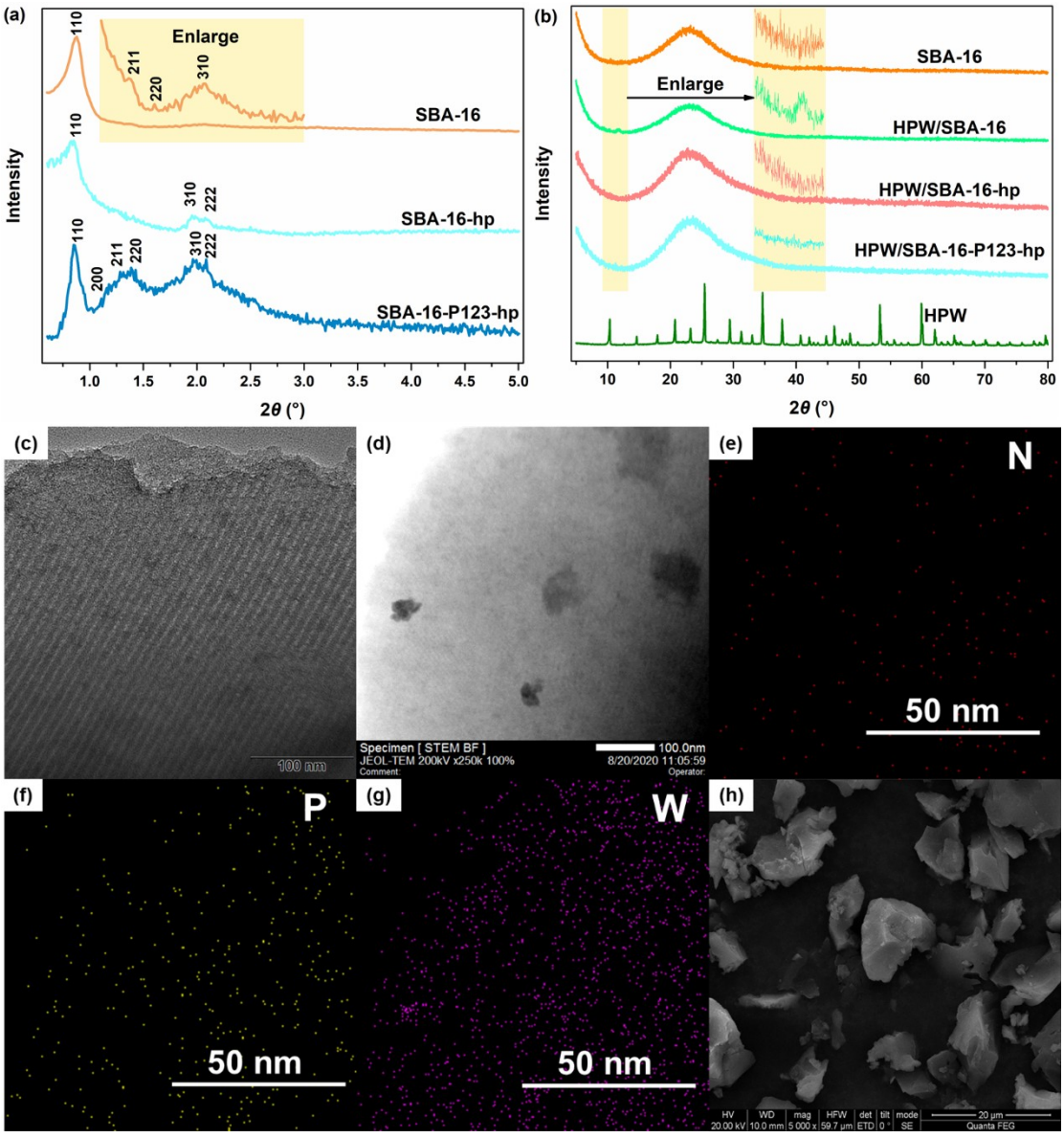

Figure 2 (a) The SAXRD images and (b) XRD images of catalysts. (c-g) TEM and elemental mapping images and (h) SEM image of HPW/SBA-16-P123-hp.

Further, the status of alkylimidazole grafted and the HPW loaded were analyzed by FT-IR. The samples after grafting show peaks at 1200~1690 cm^{-1} corresponding to stretching vibration peaks of N-C and N=C bands[36,37] (**Figure 3a**), suggesting the successful grafting of alkylimidazole. This can also be confirmed by the FT-IR results of samples after **step 1** and **step 2** in the synthesis process. As shown in **Figure S1**, the samples after **step 1** show bands at 725 cm^{-1} and 650 cm^{-1} corresponding to the stretching vibration of C-Cl band[38,39], indicating

3-chloropropyltrimethoxysilane condensed into SBA-16. The samples after **step 2** show peaks at 1200~1690 cm^{-1} belonging to N-C and N=C bands of alkylimidazole. These alkylimidazole in the surface makes HPW anchoring more tightly and evenly. As shown in **Figure 3b**, the loaded samples have bands at 989, 897 and 817 cm^{-1}, representing Keggin anions of HPW[40]. The loading amount of HPW was calculated using W content tested by ICP-OES that about 1.4 wt% for HPW/SBA-16-P123-hp, 0.6 wt% for HPW/SBA-16-hp and 0.4 wt% for HPW/SBA-16, which is in consistence with the acid amount valued by acid-base titration (1.266 mmol/g for HPW/SBA-16-P123-hp, 0.723 mmol/g for HPW/SBA-16-hp, 0.636 mmol/g for HPW/SBA-16) (**Table S1**).

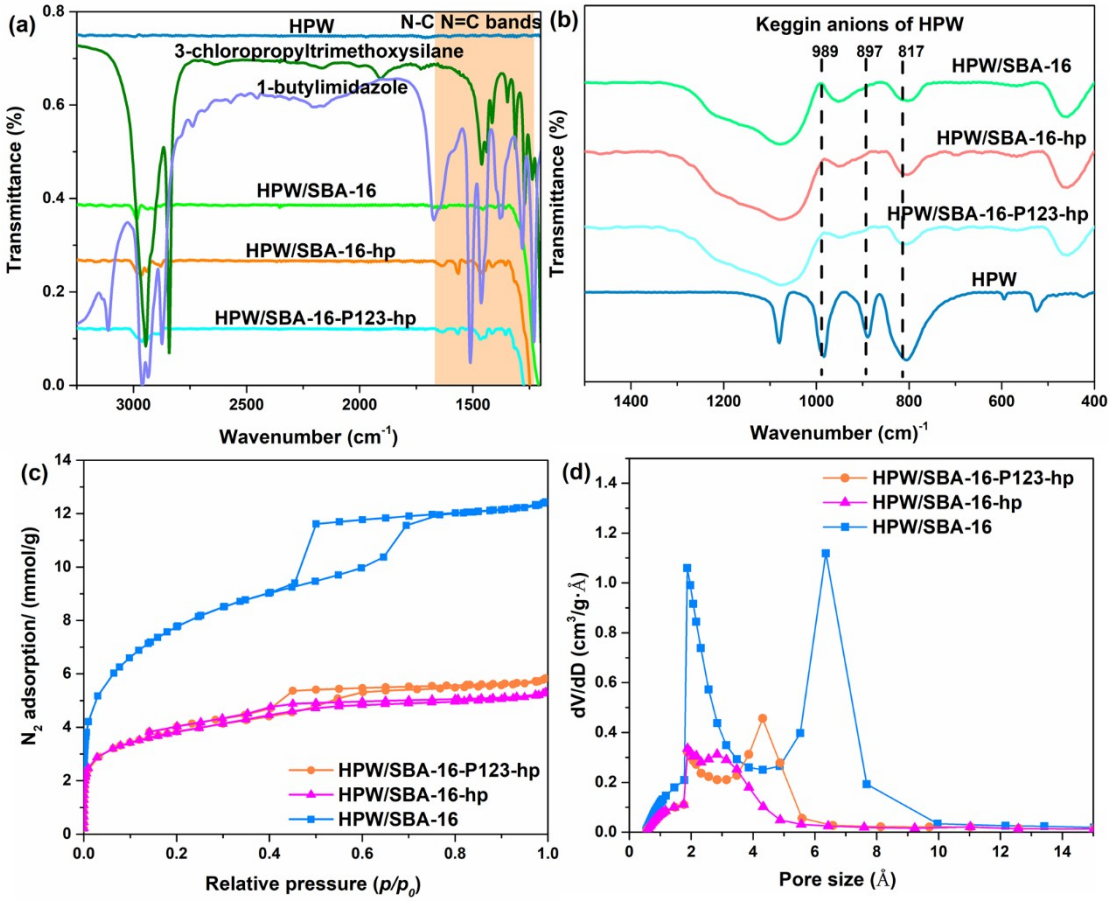

Figure 3 (a-b) FT-IR images of samples. (c) N_2 adsorption–desorption isotherm and (d) pore size distribution of catalysts.

HPW anchoring amount is also influenced by the catalyst structure. As shown in **Figure 3c-d**, samples show typical IV type curves and the H2 type hysteresis loop, indicating typical three-dimensional cage-like pore structure. These samples have pore sizes ranging from 2.0 nm to 10.0 nm with HPW/SBA-16 having the largest pore size and HPW/SBA-16-hp having the smallest ones. Conformably, HPW/SBA-16 has the largest pore volume and surface area

(620 m^2/g) and HPW/SBA-16-hp has the smallest (~290 m^2/g). This change is mainly contributed to the alkylimidazole grafted. Moreover, HPW/SBA-16-P123-hp has the larger pore size, pore volume and surface area than HPW/SBA-16-hp, which may be contributed by the co-surfactants of F127 and P123. Due to the larger surface area, HPW/SBA-16-P123-hp loads more HPW **(Table S1)**.

The influence of alkylimidazole to the thermal stability of catalysts was investigated. As shown in **Figure 4a-d**, samples after alkylimidazole grafting keep thermal stable until 328 ºC much better than the bulk HPW (210 ºC) and SBA-16 (265 ºC), suggesting alkylimidazole grafting improves the thermal stability of the catalyst. We also evaluated the grafting amount of alkylimidazole by testing the samples after **step 1** and **step 2** in the synthesis process by TG-DTG spectra respectively (**Figure S2**). After **step 1**, HPW/SBA-16-P123-hp has the similar weight loss with HPW/SBA-16-hp, meaning the similar grafting of 3-chloropropyltrimethoxysilane. After **step 2**, HPW/SBA-16-P123-hp has more weight loss than HPW/SBA-16-hp, meaning more 1-butylimidazole grafted. (**Table S2**). Of course, more HPW is immobilized on HPW/SBA-16-P123-hp.

The effect of this alkylimidazole to the hydrophobicity of samples was also studied (**Figure 4e-h**). As we know, HPW is soluble in water[41], and as it is loaded on SBA-16, the contact angle of water increases to 29.76 º, a little smaller than MSN (31.53 º). Interestingly, after alkylimidazole grafting, the contact angles of water for HPW/SBA-16-P123-hp and HPW/SBA-16-hp increase to 59.82 º and 60.69 º respectively, indicating alkylimidazole grafting enhances the hydrophobicity of samples, which improves the water tolerance of samples. As we dispersed these samples on water (**Figure 4i-l)**, HPW/SBA-16-P123-hp and HPW/SBA-16-hp are floating on the water while the HPW/SBA-16 and SBA-16 sank rapidly as soon as we put them onto the water.

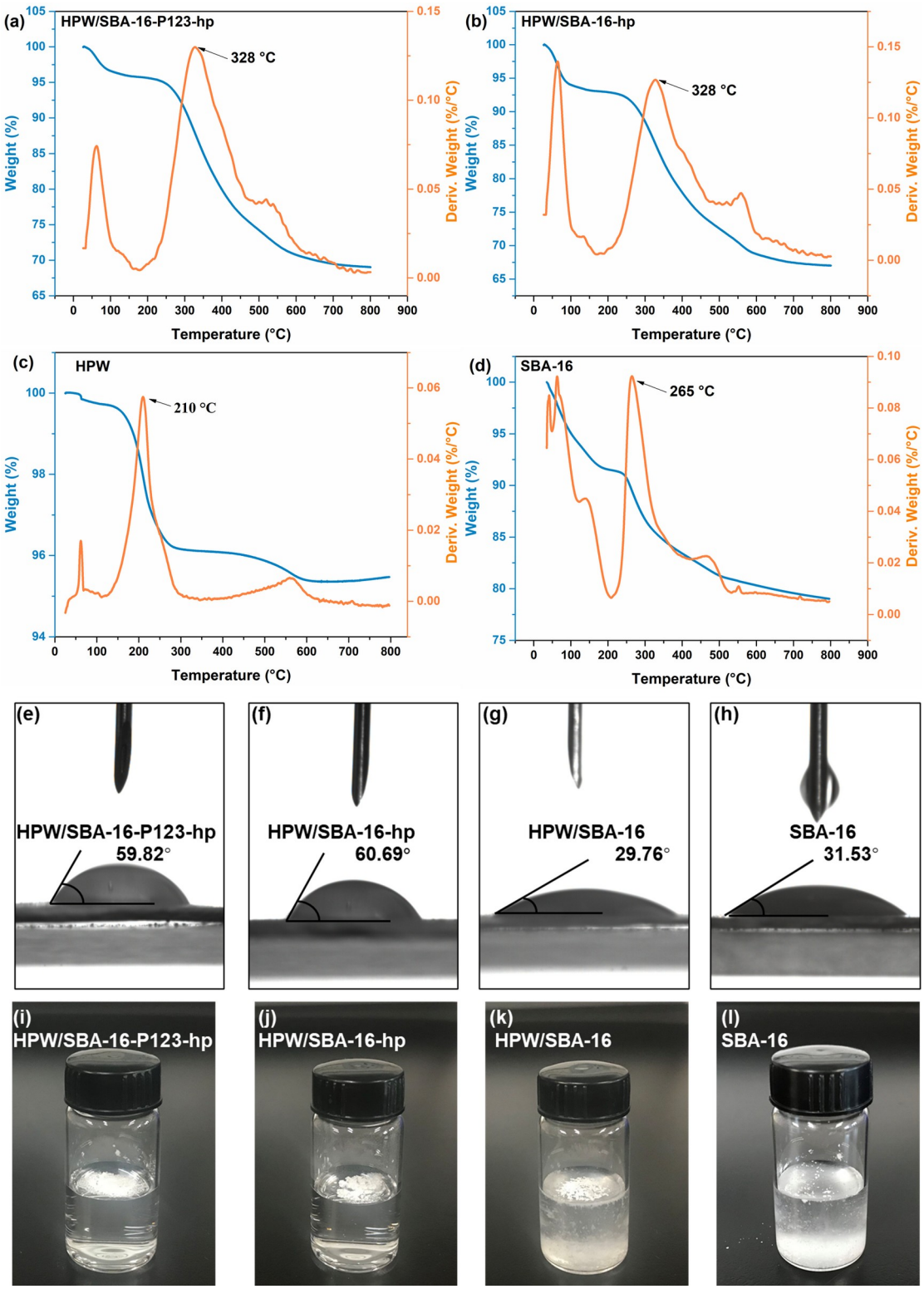

Figure 4 (a-d) TG-DTG curves of samples. (e-h) The contact angles of water for samples. (i-l) Sample dispersed statues on water.

3.2 Aldol condensation of cyclopentanone and cyclohexanone

Self-aldol condensation of cyclopentanone and self-aldol condensation of cyclohexanone

catalyzed by acid have been investigated[14]. Here, we studied the co-conversion of cyclopentanone and cyclohexanone in one-pot reaction and aimed to synthesize a fuel blending with high-performance properties (**Figure 5a**). The main products are primary-condensation and secondary-condensation products (**Figure S3**) and with time going on, the secondary-condensation products increase while the primary-condensation products go down slightly, meaning secondary-condensation products are formed based on the consumption of the primary-condensation products (**Figure S4a**).

Here a series of acid catalysts were used and the HPW/SBA-16-P123-hp has the best activity (94.9% conversion of cyclopentanone, 94.1% conversion of cyclohexanone, 64.2% yield of primary-condensation products, 27.8% yield of secondary-condensation products) and the activity of these catalysts is in consistence with the change of the acid amount, except HPW and $H_4SiW_{12}O_{40}$. Comparably, HPW/SBA-16-P123-hp shows four advantages in this reaction. Firstly, the stronger acid strength of HPW is beneficial for the condensation[41,42] that the activity of HPW (14.6% conversion of cyclopentanone, 20.6% conversion of cyclohexanone, 17.8% yield of condensed products) is higher than that of $H_4SiW_{12}O_{40}$ (5.49% conversion of cyclohexanone, 8.55% conversion of cyclohexanone, 6.99% yield of condensed products) under the similar acid amount. Secondly, loading increases the activity by increasing the efficient acid sites. As shown in **Figure 5b**, although HPW has the biggest acid amount, HPW has lower activity than the loaded ones[41] that the yield of condensed products is only about 17.84%. As it was loaded on SBA-16, the yield of products is improved to 22.9% and as it was loaded on SBA-16-P123-hp, the yield of products is improved to 91.9%. Thirdly, the confined environment inhibits the secondary-condensation products by mass transfer resistance, which is very advantageous for the synthesis of low-freezing point products. Comparing with the result by the same amount of HPW (**Figure S4b**), the secondary-condensation products yield decreases from 43.0% to 27.8%. Fourthly and the most importantly, this catalyst has high stability, which is contributed to improved water tolerance by creating relative hydrophobic environment by grafting alkylimidazole. After reaction, samples were centrifuged and washed by dichloromethane, dried at 60 ^{o}C for 12 h and used for the next reaction. In the case of reaction using HPW/SBA-16-hp, the conversion

of reactants and selectivity of products are almost unchanged after consecutive 5 runs. In contrast, in the case of reaction by HPW/SBA-16, the conversions of reactants decrease obviously just after one run (**Figure 5c**).

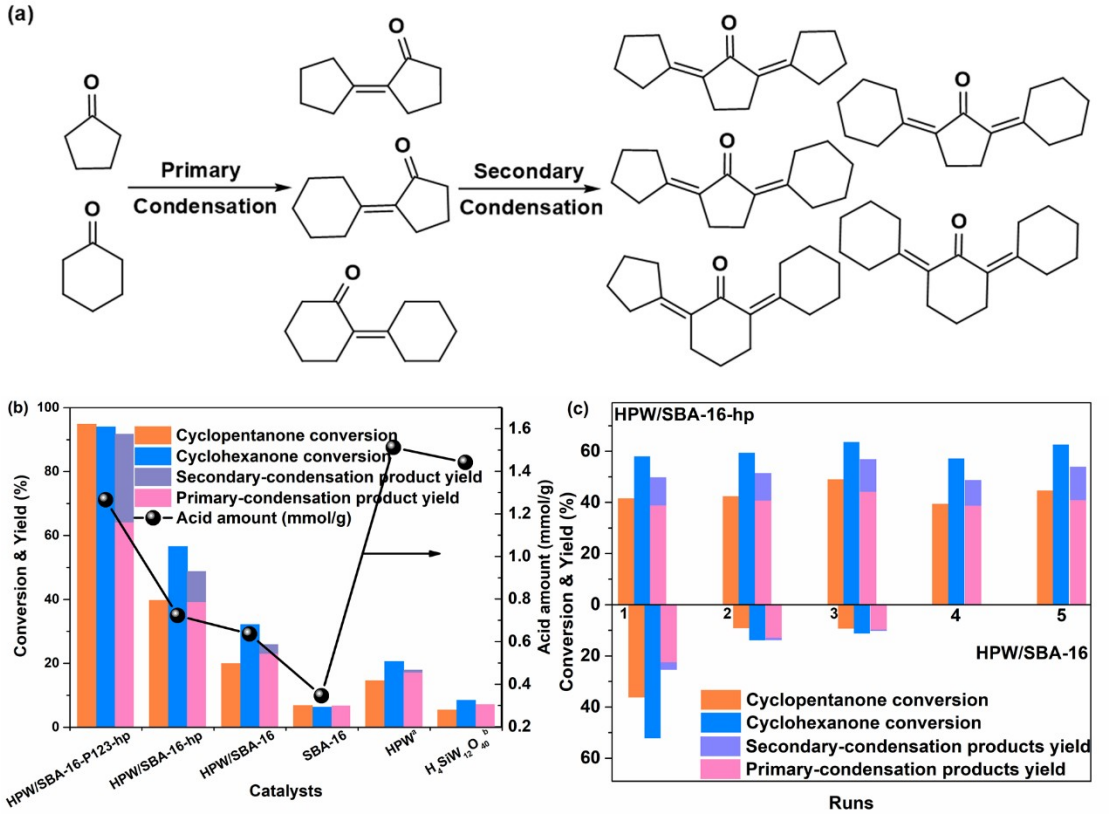

Figure 5 (a) Synthesis of jet fuel blending using cyclopentanone and cyclohexanone. (b) The aldol reaction of cyclopentanone and cyclohexanone with different catalysts and (c) the recycle reactions of cyclopentanone and cyclohexanone with HPW/SBA-16-hp and HPW/SBA-16, respectively. Reaction condition: 8.14 g cyclopentanone, 9.50 g cyclohexanone and 1.0 g catalyst, 160 °C, 32 h. a, b: The catalyst amount is same with the HPW loaded on the other catalysts.

3.3 Properties of synthesized fuel blending

The condensation products by HPW/SBA-16-P123-hp were hydrodeoxygenated, and we obtained a fuel blending (***Fuel 1,*** **entry 1 in Table 1**) composed of about 67.7% of primary-condensation fuel and 32.3% secondary-condensation fuel. This fuel blending has density of about 0.905 g/mL, NHOC of 42.73 MJ/kg, freezing point of -67 °C and kinematic viscosity of 7.61 mm^2/s (20 °C) satisfying the requirement as jet fuel. In order to analyze the excellent properties of this fuel blending, we obtained primary-condensation fuel (***Fuel 2,*** **entry 2 in**

Table 1) and secondary-condensation fuel (***Fuel 3,*** **entry 3 in Table 1**) by vacuum distillation. ***Fuel 2*** has excellent freezing point (about -54 °C) and good density (about 0.878 g/mL), which is much better than fuels from self-condensation of cyclic ketones (**entry 4 and 5**), contributing to property balance by the unsymmetrical composition[6] (**entry 6**). ***Fuel 3*** has excellent density about 0.940 g/mL comparable to JP-10, but the viscosity is a little higher (about 68.86 mm^2/s at 20 °C). Comparing these fuels, ***Fuel 1*** takes the advantages of good low-temperature properties of ***Fuel 2*** and the high density of ***Fuel 3***, suggesting cross-condensation of cyclopentanone and cyclohexanone is a good method to make high-performance jet fuels.

Table 1 Properties of biofuels synthesized in this work and literatures.

Entry	Hydrocarbon	Feedstock	Density at 20 °C (g/mL)	Kinematic viscosity (20 °C) (mm^2/s)	Freezing point (°C)	NHOC (MJ/kg)	Ref.
1	*Fuel 1*	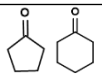	0.905	7.61	<-67	42.73	This work
2	*Fuel 2*[a]		0.878	3.13	-54	42.99	This work
3	*Fuel 3*		0.940	68.86	-50	42.48	This work
4	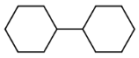		0.886	3.72 (25 °C)	2.6	42.42	[43,14]
5	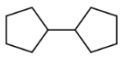		0.867	1.62 (25 °C)	-38	42.97	[14]
6	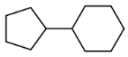		0.880	2.0	<-75	-	[6]

[a] 7.61%  , 49.06%  , 40.37% 

4. Conclusions

We developed a highly stable, efficient, and water-tolerant SBA-16 confined HPW catalyst and used it to controllably catalyze the condensation of cyclopentanone and cyclohexanone to synthesize high-performance bio-jet fuel blending. SBA-16 was synthesized by hydrothermal method and surface is modified using imidazolium halogenides. HPW is loaded in the channels of the SBA-16 by anion exchange with imidazolium halogenides. The alkylimidazole improves the stability of catalyst by creating relative

hydrophobic environment and leads to activity almost unchanged in 5 runs. The pore size is controlled by alkylimidazole grafting and surfactants used, and it affects the products distribution with about 64.2% yield of primary-condensation and 27.8% yield of secondary-condensation products produced. After hydrodeoxygenation, a high-performance fuel blending was obtained with density of about 0.905 g/mL, NHOC of 42.73 MJ/kg, freezing point of -67 ^{o}C and kinematic viscosity of 7.61 mm^2/s (20 ^{o}C), contributing to the balance of different compositions. This study provides a promising route for synthesizing high-performance jet fuel from lignocellulose and suggests a highly efficient and stable catalyst in the shape-selective reaction involving acid water produced.

Conflicts of interest

There are no conflicts to declare.

Acknowledgments

The authors appreciate the supports from the National Natural Science Foundation of China (21808162); National Postdoctoral Program for Innovative Talents (BX20180212) and China Postdoctoral Science Foundation (2018M631743).

References

1. Jing Y, Guo Y, Xia Q, Liu X and Wang Y. Catalytic production of value-added chemicals and liquid fuels from lignocellulosic biomass. *Chem*. 2019.
2. Yang J, Xin Z, He Q, Corscadden K and Niu H. An overview on performance characteristics of bio-jet fuels. *Fuel*. 2019;237:916-936.
3. Li N, Wang J-G, Xu J-X, Liu J-Y, Zhou H-J, Sun P-C and Chen T-H. Synthesis of hydrothermally stable, hierarchically mesoporous aluminosilicate Al-SBA-1 and their catalytic properties. *Nanoscale*. 2012;4:2150-2156.
4. Nie G, Zhang X, Han P, Xie J, Pan L, Wang L and Zou J-J. Lignin-derived multi-cyclic high density biofuel by alkylation and hydrogenated intramolecular cyclization. *Chemical Engineering Science*. 2017;158:64-69.
5. Li Z, Pan L, Nie G, Xie J, Xie J, Zhang X, Wang L and Zou J-J. Synthesis of high-performance jet fuel blends from biomass-derived 4-ethylphenol and phenylmethanol. *Chemical Engineering Science*. 2018;191:343-349.
6. Nie G, Dai Y, Liu Y, Xie J, Gong S, Afzal N, Zhang X, Pan L and Zou J-J. High yield one-pot synthesis of high density and low freezing point jet-fuel-ranged blending from bio-derived phenol and cyclopentanol. *Chemical Engineering Science*. 2019;207:441-447.
7. Liu Y, Li G, Hu Y, Wang A, Lu F, Zou J-J, Cong Y, Li N and Zhang T. Integrated conversion of cellulose to high-density aviation fuel. *Joule*. 2019;3:1028-1036.
8. Nie G, Zou J-J, Feng R, Zhang X and Wang L. HPW/MCM-41 catalyzed isomerization and dimerization of pure pinene and crude turpentine. *Catalysis Today*. 2014;234:271-277.

9. Li Z, Wang Y and Wang H. Development of intermediates for high-energy content new biomass-derived jet and diesel fuels with a robust rapid green reaction. *Energy Technology*. 2019;7:1900418.
10. Li G, Hou B, Wang A, Xin X, Cong Y, Wang X, Li N and Zhang T. Making JP-10 superfuel affordable with a lignocellulosic platform compound. *Angewandte Chemie*. 2019;131:12282-12286.
11. Hronec M, Fulajtárova K, Liptaj T, Štolcová M, Prónayová N and Soták T. Cyclopentanone: A raw material for production of C15 and C17 fuel precursors. *Biomass and Bioenergy*. 2014;63:291-299.
12. Xie J, Zhang L, Zhang X, Han P, Xie J, Pan L, Zou D-R, Liu S-H and Zou J-J. Synthesis of high-density and low-freezing-point jet fuel using lignocellulose-derived isophorone and furanic aldehydes. *Sustainable Energy & Fuels*. 2018;2:1863-1869.
13. Sacia E R, Balakrishnan M, Deaner M H, Goulas K A, Toste F D and Bell A T. Highly selective condensation of biomass-derived methyl ketones as a source of aviation fuel. *ChemSusChem*. 2015;8:1726-1736.
14. Deng Q, Nie G, Pan L, Zou J-J, Zhang X and Wang L. Highly selective self-condensation of cyclic ketones using MOF-encapsulating phosphotungstic acid for renewable high-density fuel. *Green Chemistry*. 2015;17:4473-4481.
15. Dai Y, Nie G, Gong S, Wang L, Pan L, Fang Y, Zhang X and Zou J-J. Reduced graphene oxide enhanced emulsification for one-pot synthesis of high-density jet fuel. *Fuel*. 2020;275:117962.
16. Chang H, Motagamwala A H, Huber G W and Dumesic J A. Synthesis of biomass-derived feedstocks for the polymers and fuels industries from 5-(hydroxymethyl)furfural (HMF) and acetone. *Green Chemistry*. 2019;21:5532-5540.
17. Xu Q, Zhang L, Sun K, Shao Y, Tian H, Zhang S, Liu Q, Hu G, Wang S and Hu X. Cross-polymerisation between the model furans and carbohydrates in bio-oil with acid or alkaline catalysts. *Journal of the Energy Institute*. 2020;93:1678-1689.
18. Yang J, Li N, Li G, Wang W, Wang A, Wang X, Cong Y and Zhang T. Solvent-free synthesis of c10 and c11 branched alkanes from furfural and methyl isobutyl ketone. *Chemsuschem*. 2013;6:1149-1152.
19. Yang G, Jiang J Q and Zhang Y W. Synthesis of cyclohexanone-formaldehyde resin catalyzed by rehydrated Mg-Al hydrotalcite. *Progress in Organic Coatings*. 2015;78:55-58.
20. Xia Q-N, Cuan Q, Liu X-H, Gong X-Q, Lu G-Z and Wang Y-Q. Pd/NbOPO4 multifunctional catalyst for the direct production of liquid alkanes from aldol adducts of furans. *Angewandte Chemie International Edition*. 2014;53:9755-9760.
21. Zhao L, An H, Zhao X and Wang Y. TiO2-catalyzed n-valeraldehyde self-condensation reaction mechanism and kinetics. *ACS Catalysis*. 2017;7:4451-4461.
22. Wan M, Liang D, Wang L, Zhang X, Yang D and Li G. Cycloketone condensation catalyzed by zirconia: Origin of reactant selectivity. *Journal of Catalysis*. 2018;361:186-192.
23. Ramos R, Hidalgo J M, Göpel M, Tišler Z, Bertella F, Martínez A, Kikhtyanin O and Kubička D. Catalytic conversion of furfural-acetone condensation products into bio-derived C8 linear alcohols over NiCu/Al-SBA-15. *Catalysis Communications*. 2018;114:42-45.
24. Cho H J, Kim D, Li J, Su D and Xu B. Zeolite-encapsulated Pt nanoparticles for tandem catalysis. *Journal of the American Chemical Society*. 2018;140:13514-13520.
25. Zuo C, Ge T, Guo X, Li C and Zhang S. Synthesis and catalytic performance of Cs/P modified ZSM-5 zeolite in aldol condensation of methyl acetate with different sources of formaldehyde. *Microporous and Mesoporous Materials*. 2018;256:58-66.
26. Busca G. Acid catalysts in industrial hydrocarbon chemistry. *Chemical Reviews*. 2007;107:5366-

5410.
27. Zhang X, Deng Q, Han P, Xu J, Pan L, Wang L and Zou J-J. Hydrophobic mesoporous acidic resin for hydroxyalkylation/alkylation of 2-methylfuran and ketone to high-density biofuel. *AIChE Journal*. 2017;63:680-688.
28. Vijayakumar G and Pandurangan A. Up-gradation of α-tetralone to jet-fuel range hydrocarbons by vapour phase hydrodeoxygenation over PdNi/SBA-16 catalysts. *Energy*. 2017;140:1158-1172.
29. Deng Q, Han P, Xu J, Zou J-J, Wang L and Zhang X. Highly controllable and selective hydroxyalkylation/alkylation of 2-methylfuran with cyclohexanone for synthesis of high-density biofuel. *Chemical Engineering Science*. 2015;138:239-243.
30. Inumaru K, Ishihara T, Kamiya Y, Okuhara T and Yamanaka S. Water-Tolerant, Highly Active Solid Acid Catalysts Composed of the Keggin-Type Polyoxometalate H3PW12O40 Immobilized in Hydrophobic Nanospaces of Organomodified Mesoporous Silica. *Angewandte Chemie International Edition*. 2007;46:7625-7628.
31. Karimi B and Vafaeezadeh M. SBA-15-functionalized sulfonic acid confined acidic ionic liquid: a powerful and water-tolerant catalyst for solvent-free esterifications. *Chemical Communications*. 2012;48:3327-3329.
32. Sofia L T A, Krishnan A, Sankar M, Raj N K K, Manikandan P, Rajamohanan P R and Ajithkumar T G. Immobilization of Phosphotungstic Acid (PTA) on Imidazole Functionalized Silica: Evidence for the Nature of PTA Binding by Solid State NMR and Reaction Studies. *Journal of Physical Chemistry C*. 2009;113:21114-21122.
33. He S, Liu S, Dai W, Zhai S and Lin J. Nanocomposite Proton Exchange Membranes Incorporating Phosphotungstic Acid Anchored on Imidazole-Functionalized Halloysite Nanotubes. *Journal of the Electrochemical Society*. 2018;165:F951-F958.
34. Dorado F, Romero R and Cañizares P. Hydroisomerization of n-butane over Pd/HZSM-5 and Pd/Hβ with and without binder. *Applied Catalysis A: General*. 2002;236:235-243.
35. Zhao D, Huo Q, Feng J, Chmelka B F and Stucky G D. Nonionic Triblock and Star Diblock Copolymer and Oligomeric Surfactant Syntheses of Highly Ordered, Hydrothermally Stable, Mesoporous Silica Structures. *Journal of the American Chemical Society*. 1998;120:6024-6036.
36. Özyalçın M and Küçükyavuz Z. Synthesis, characterization and electrical properties of iodinated poly(N-vinylimidazole). *Synthetic Metals*. 1997;87:123-126.
37. Yao K, Wang Z, Wang J and Wang S. Biomimetic material—poly(N-vinylimidazole)–zinc complex for CO2 separation. *Chemical Communications*. 2012;48:1766-1768.
38. Jaramillo D M, Hunka D E and Land D P. Thermal Chemistry of cis-1,2-Dichloroethene on Pd(111). *Langmuir*. 2004;20:5782-5785.
39. Gao J and Teplyakov A V. Thermal transformations of 2-chlorophenol on a surface of ZnO powder catalyst. *Catalysis Today*. 2014;238:111-117.
40. Staiti P, Freni S and Hocevar S. Synthesis and characterization of proton-conducting materials containing dodecatungstophosphoric and dodecatungstosilic acid supported on silica. *Journal of Power Sources*. 1999;79:250-255.
41. Kozhevnikov I V. Catalysis by Heteropoly Acids and Multicomponent Polyoxometalates in Liquid-Phase Reactions. *Chemical Reviews*. 1998;98:171-198.
42. Al-Faze R, Finch A, Kozhevnikova E F and Kozhevnikov I V. Dehydration of methanol and ethanol over silica-supported heteropoly acids in the gas phase: Surface-type versus bulk-type catalysis mechanism. *Applied Catalysis A: General*. 2020;597:117549.

43. Jiang X, He G, Wu X, Guo Y, Fang W and Xu L. Density, Viscosity, Refractive Index, and Freezing Point for Binary Mixtures of 1,1′-Bicyclohexyl with Alkylcyclohexane. *Journal of Chemical & Engineering Data*. 2014;59:2499-2504.